

## Magneto-optical imaging of transient vortex states in superconductors

D. Giller, B. Kalisky, and A. Shaulov

*Institute of Superconductivity, Bar-Ilan University, Ramat-Gan 52900, Israel*

T. Tamegai

*Department of Applied Physics, The University of Tokyo, Hongo, Bunkyo-ku, Tokyo 113-8656, Japan*

Y. Yeshurun<sup>a)</sup>

*Institute of Superconductivity, Bar-Ilan University, Ramat-Gan 52900, Israel*

A high temporal resolution magneto-optical system is employed to follow the crystallization process of the quasiordered vortex state in  $\text{Bi}_2\text{Sr}_2\text{CaCu}_2\text{O}_{8+\delta}$  crystals following a sudden change in the applied magnetic field. Two types of experiments are performed. In the first one the sample is suddenly exposed to a steady magnetic field smaller than the vortex order–disorder transition field,  $B_{od}$ . In the second type of experiment the sample is initially exposed to an external field larger than  $B_{od}$ , and then the field is suddenly reduced. The two types of experiments reveal growth of the quasiordered state proceeding in opposite directions: from the sample center toward its edge in the first experiment, and from the sample edge toward the center in the second experiment. This motion enables tracing of the time evolution of the thermodynamic quasiordered vortex phase in the early stages of its formation. © 2001 American Institute of Physics. [DOI: 10.1063/1.1356044]

Magneto-optical (MO) imaging utilizing ferrimagnetic iron–garnet indicators with in-plane anisotropy has emerged as a powerful technique in the study of the vortex matter in high temperature superconductors (HTS).<sup>1–5</sup> In this technique, an iron–garnet indicator film is placed in intimate contact with the surface of the sample. Linearly polarized light, reflected from a mirror coating the back surface of the indicator film, undergoes a double Faraday rotation in the indicator film. The light is then passed through an analyzer, yielding a two-dimensional real time image in which the local light intensity is determined by the local magnetic field at the sample surface. Thus this technique allows a direct observation of flux penetration and induction distribution in superconductors. Typical spatial resolution of this method is a few micrometers, and typical field resolution is a few gauss.

Recently, we constructed a MO system with enhanced time resolution for the study of dynamic magnetic properties of HTS. Introducing a high speed digital charge coupled device camera (Hamamatsu 4880-80) enables the capturing of 25 high-quality full frames per second. From these images, one-dimensional profiles (induction versus position) across the sample width are extracted. We have employed this system to study the crystallization process of the quasiordered vortex state in a  $1.5 \times 0.7 \times 0.03 \text{ mm}^3$   $\text{Bi}_2\text{Sr}_2\text{CaCu}_2\text{O}_{8+\delta}$  (BSCCO) crystal<sup>6</sup> after a sudden change of the applied magnetic field. This crystallization process has been investigated in two types of experiments. In the first one, “field-step-up” experiment, the sample is suddenly exposed to a steady magnetic field  $B_a$  smaller than the vortex order–disorder transition field,  $B_{od} \approx 450 \text{ G}$ . In the second type of experiment, “field-step-down,” the sample is initially exposed to an external field larger than  $B_{od}$  for a long enough time to allow for the establishment of an equilibrium disordered state. Then,

the field is suddenly reduced to a value below  $B_{od}$ . The two types of experiments reveal growth of the quasiordered state proceeding in opposite directions. In this article we describe the experimental data and interpret them as revealing the nucleation and growth process of the quasiordered vortex phase.

Figure 1 shows the time evolution of the magnetic induction profiles at  $T=20 \text{ K}$  after a step increase (rise time  $\approx 50 \text{ ms}$ ) of the external magnetic field from 0 to 380 G. The time elapse between subsequent profiles is 100 ms. As indicated by the profiles, the induction at the sample edge,  $B_a \approx 300 \text{ G}$ , is well below  $B_{od}$ . Initially, Bean-type profiles are observed, gradually evolving into equilibrium dome-shaped profiles. The sharp induction step at the edges is due to surface currents  $j_s$ .<sup>2</sup> Assuming, in addition to  $j_s$ , a uniform bulk current density  $j_b$ , the profiles of Fig. 1 may be fitted to the Biot–Savart law. Thus one may conclude that the profiles of Fig. 1 describe the time evolution of a single

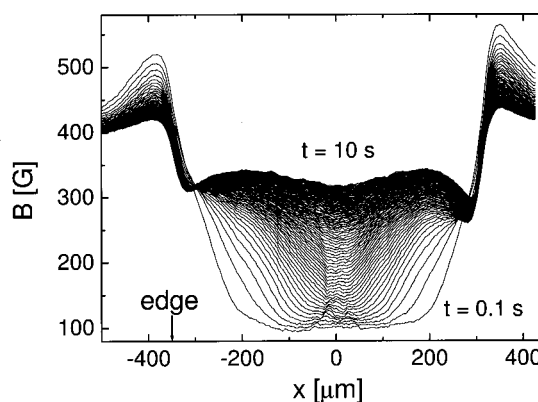


FIG. 1. Time evolution of the magnetic induction profiles in BSCCO at  $T = 20 \text{ K}$ , after a step increase of the external magnetic field, from 0 to 380 G. The time elapsed between subsequent profiles is 100 ms.

<sup>a)</sup>Electronic mail: yeshurun@mail.biu.ac.il

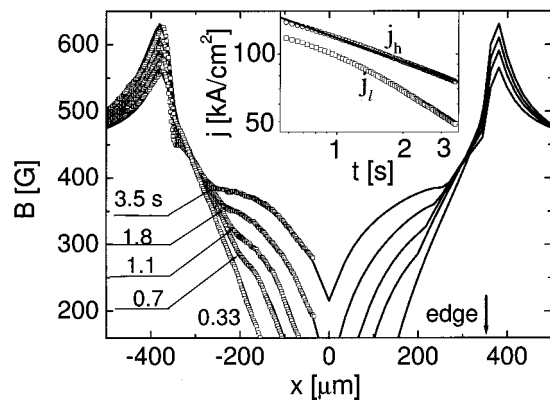


FIG. 2. Time evolution of the magnetic induction profiles at  $T=20$  K, after a step increase of the external magnetic field, from 0 to 450 G. Arrows denote the location  $x_f$  of the breaks in the profiles. Solid lines are fits obtained using the Biot-Savart law. Inset: Time dependence of the bulk currents  $j_l$  (squares) and  $j_h$  (circles). The solid line is a power-law fit to  $j_h(t)$ .

vortex phase, namely the quasiordered phase characterized by the equilibrium dome-shaped profile.

Figure 2 shows the time evolution of the magnetic induction profiles at 20 K, after a step increase of the external magnetic field, from 0 to 450 G. The induction at the sample edge is now closer to  $B_{od}$ . For clarity we show here only a few profiles, captured at the indicated times. A remarkable feature in the figure is the sharp change in the slope of the induction profiles at  $x=x_f$ , indicating a change in the bulk current density, which appears about 0.5 s after abrupt application of a magnetic field. As evident from the figure, after its appearance the point  $x_f$  moves progressively with time toward the sample edges and, simultaneously, the induction  $B_f$  at  $x_f$  increases. In contrast to the profiles shown in Fig. 1, the profiles of Fig. 2 cannot be fitted to the Biot-Savart law using a uniform bulk current density. However, assuming two different values,  $j_h$  and  $j_l$ , for the bulk current densities on both sides of  $x_f$ , one obtains excellent fits as shown by the solid lines in Fig. 2. As shown in the log-log plot in the inset, the bulk current  $j_h$ , corresponding to the part of the profile near the edges, exhibits power-law decay with time ( $j_h \propto t^{-0.35}$ ), whereas deviations from a power-law are evident for  $j_l$ .

The break in the profile at  $x_f$ , which marks changes in the bulk current density and in the relaxation characteristics, indicates a dynamic coexistence of two distinct vortex states on both sides of  $x_f$ . The experimental data find a natural explanation assuming that the *sudden* injection of vortices into the sample through the inhomogeneous surface barriers creates a transient disordered state of the vortex matter.<sup>7</sup> Subsequent to the injection of the transient disordered state, a quasiordered vortex state starts to nucleate near the sample center where the field is minimum. The growth of this state, as dictated by the thermodynamic conditions, leads to the coexistence of two states with different characteristics: An ordered state in the sample interior and a disordered state near the edges. Consistent with this picture we observe larger persistent currents and slower relaxation near the edges, indicating a disordered state. The observed break in the profile

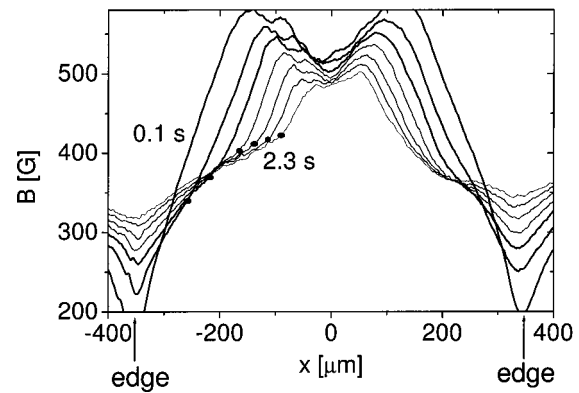


FIG. 3. Time evolution of the magnetic induction profiles at  $T=20$  K, after a step decrease of the external magnetic field, from 660 to 330 G at  $t = 0.1, 0.26, 0.46, 0.7, 1.06, 1.54,$  and  $2.3$  s. Bold circles indicate the breaks in the profiles.

at  $x_f$ , marked by the border between these two phases, can be viewed as the front of the growing quasiordered phase. The motion of the front toward the edges is now well-understood. Since in this case  $B_f$  is always smaller than  $B_{od}$ , the ordered state progressively expands toward the sample edges, as dictated by the thermodynamic conditions.

The absence of traces of the transient disordered state in the data of Fig. 1 can be explained on the basis of the observation<sup>4</sup> that the lifetime of the transient state increases as the induction at  $x_f$  approaches  $B_{od}$ . Since  $B_a$  in Fig. 1 is well below  $B_{od}$ , the lifetime of the transient state is shorter than our time resolution. In order to observe the transient state, the field must be raised to values closer to  $B_{od}$ , as in Fig. 2.

Dynamic coexistence of quasiordered and disordered states can also be observed in field-step-down experiments in which the field is suddenly reduced. In a typical experiment we apply a field of 660 G (larger than  $B_{od}$ ) and wait a long enough time for the establishment of a thermodynamic disordered state in the entire sample. This is manifested by the absence of breaks in the profiles.<sup>4</sup> When this stage is reached, the field is reduced abruptly to 330 G (below  $B_{od}$ ). As shown in Fig. 3, the profiles in this experiment also exhibit a break point  $x_f$ . However, in this case, the break point proceeds toward the sample center. Yet, these results can be interpreted in a similar way. When the field is reduced, the induction profile is partially inverted, causing part of the profile, near the edges, to drop below  $B_{od}$ . The induction is minimum at the edges, thus the ordered phase nucleates at the edges and propagates toward the sample center. At the same time, due to magnetic relaxation, the central part of the profile decreases below  $B_{od}$ , allowing the growth of the quasiordered state throughout the entire sample.

We also performed field-step-down experiments where the sample was initially exposed to a field *smaller* than  $B_{od}$ . After waiting a long enough time for the establishment of the quasiordered state in the entire sample, indicated by the appearance of a dome-shaped profile, the field was then abruptly reduced. Despite the rapid change in the field we were not able, so far, to detect breaks in the profiles; all the profiles measured after the field change were smooth, indi-

cating homogeneous bulk current. This is to be contrasted with the breaks in the profiles of Fig. 3, where the initial field was larger than  $B_{od}$ . A possible explanation for these different results may be based on the observation that the lifetime of the transient state is shorter for smaller applied fields.<sup>4</sup> We thus argue that even when the field is reduced from an initial state below  $B_{od}$ , a transient disordered state is created, but its lifetime is shorter than our experimental time window. This explanation is analogous to that given above for the absence of breaks in the profiles of Fig. 1 measured after an abrupt field-step-up. We note, however, that surface barriers may play a different role in field-step-up and field-step-down experiments.<sup>8</sup> Based on this asymmetry in the effect of the surface barrier we propose an alternative explanation to the absence of breaks in the profiles after reducing the field from  $B_a < B_{od}$ : When vortices exit the sample, surface barriers are ineffective in creating a transient disordered state. Thus it is possible that if the initial state is quasiordered, it will transform continuously to the equilibrium quasiordered state without going through an intermediate disordered state. Only if the initial state is disordered, i.e.,  $B_a > B_{od}$ , dynamic coexistence of disordered and quasiordered states may be observed.

In conclusion, a necessary condition to observe a front of a growing quasiordered phase in field-step-up experiments is the creation of a transient disordered state with a long enough lifetime. This is accomplished by increasing the field

to a value close to  $B_{od}$ . In field-step-down experiments a front can be observed when the initial state is disordered. It is yet unclear to us whether the front may be observed also in field-step-down experiments when the initial state is ordered.

This work was supported by the Israel Science Foundation (ISF)—Excellence Center Program and by the Heinrich Hertz Minerva Center for High Temperature Superconductivity. Y.Y. acknowledges support from the U.S.–Israel Binational Science Foundation. A.S. acknowledges support from the ISF. D.G. acknowledges support from the Clore Foundation. T.T. acknowledges support from a Grant-in-Aid for Scientific Research from the Ministry of Education, Science, Sports and Culture, and from CREST.

<sup>1</sup>For a review see: V. K. Vlasko-Vlasov *et al.*, NATO Adv. Study Inst. Ser., Ser. E **356**, 205 (1999); A. A. Polyanskii *et al.*, NATO ASI Ser., Ser. 3 **72**, 353 (1999); M. R. Koblischka and R. J. Wijngaarden, *Supercond. Sci. Technol.* **8**, 199 (1995).

<sup>2</sup>M. V. Indenbom *et al.*, *Physica C* **222**, 203 (1994).

<sup>3</sup>A. Soybel *et al.*, *Nature (London)* **406**, 282 (2000).

<sup>4</sup>D. Giller *et al.*, *Phys. Rev. Lett.* **84**, 3698 (2000); D. Giller *et al.*, *Physica B* **284–8**, 699 (2000); D. Giller *et al.*, *Physica C* **341–8**, 987 (2000).

<sup>5</sup>C. J. van der Beek *et al.*, *Phys. Rev. Lett.* **84**, 4196 (2000); C. J. van der Beek *et al.*, *Physica C* **341–8**, 1319 (2000).

<sup>6</sup>N. Motohira *et al.*, *J. Ceram. Soc. Jpn.* **97**, 994 (1989).

<sup>7</sup>Y. Paltiel *et al.*, *Nature (London)* **403**, 398 (2000); Y. Paltiel *et al.*, *Phys. Rev. Lett.* **85**, 3712 (2000).

<sup>8</sup>L. Burlachkov *et al.*, *J. Appl. Phys.* **70**, 5759 (1991).